Available online at www.CivileJournal.org

Civil Engineering Journal

(E-ISSN: 2476-3055; ISSN: 2676-6957)

Vol. 7, Special Issue, 2021

"Innovative Strategies in Civil Engineering Grand Challenges"

Effect of Liquefaction Induced Lateral Spreading on Seismic Performance of Pile Foundations

G. M. Basavana Gowda [1*], S. V. Dinesh [2], L. Govindaraju [3], R. Ramesh Babu [4]

[1] *Department of Civil Engineering, Ramaiah Institute of Technology, Karnataka 560054, India.*

[2] *Department of Civil Engineering, Siddaganga Institute of Technology, Tumakuru, India*

[3] *University Visvesvaraya College of Engineering (UVCE), Bangalore, India.*

[4] *Central Power Research Institute, Bangalore, India.*

Received 24 October 2021; Revised 09 February 2022; Accepted 22 February 2022; Published 12 March 2022

Abstract

Seismically active areas are vulnerable to liquefaction, and the influence of liquefaction on pile foundations is very severe. Study of pile-supported buildings in liquefiable soils requires consideration of soil-pile interaction and evaluation of the interaction resulting from movement of soil surrounding the pile. This paper presents the results of three-dimensional finite difference analyses conducted to understand the effect of liquefiable soils on the seismic performance of piles and pile groups embedded in stratified soil deposits using the numerical tool FLAC3D. A comparative study has been conducted on the performance of pile foundations on level ground and sloping ground. The soil model consists of a non-liquefiable, slightly cemented sand layer at the top and bottom and a liquefiable Nevada sand layer in between. This stratified ground is subjected to 1940 El Centro, 2001 Bhuj (India) earthquake ground motions, and harmonic motion of 0.3g acceleration. Parametric studies have been carried out by changing the ground slope from 0° to 10° to understand the effects of sloping ground on pile group response. The results indicate that the maximum bending moments occur at boundaries between liquefiable and non-liquefiable layers, and that the bending moment increases with an increase in slope angle. The presence of a pile cap prevents horizontal ground displacements at ground level. Further, it is also observed that the displacements of pile groups under sloping ground are in excess of those on level ground due to lateral spreading.

Keywords: FLAC3D; Pile Foundations; Earthquake; Soil-pile Interaction.

1. Introduction

Pile foundations are generally recommended when the soil strata are poor at shallow depths in terms of their bearing capacity. When an earthquake strikes, pore water pressure rises in saturated sandy soils, the soil deposit becomes a fluidized bed and is said to be liquefied, resulting in loss of strength, stiffness, and reduction of modulus of the soil. Liquefaction causes instability, leading to damage of the facilities and structures. It can also cause severe damage to piles of bridges during seismic excitations. Centrifuge studies [1-6] have shown that the bending moment in a pile increases due to the existence of a pile cap caused by the densification of soil surrounding the piles. The maximum moment develops at the bottom of liquefiable strata at the end of shaking in a three-layered soil for end-bearing piles. In the case of sloping grounds, the movement of soil exerts increased lateral pressure on piles, which leads to their failure. The behavior of the pile foundation under earthquake excitation decides the performance of the superstructure above the piles.

* Corresponding author: basavanagowda@msrit.edu

http://dx.doi.org/10.28991/CEJ-SP2021-07-05

Soil that suffers the loss of strength and stiffness owing to the rise of excess pore water pressure during liquefaction results in the maximum bending moment and shear force induced in piles. When soil losses its strength and stiffness, the pile acts as a slender column and the liquefied soil around the pile exerts more stress than the yield stress, resulting in an increase in lateral deflection and the formation of the plastic hinges at several locations along the depth of the pile [7, 8]. Phanikanth et al. (2013) [9] have reported the effect of sloping ground on piles varying from 10% to 40%. They have observed an amplification factor of 1.6 for non-dimensional deflection and bending moment co-efficient when slope varies from 10% to 40%. However, with respect to liquefiable soil, the amplification factor for the peak bending moment of the pile is 2.5 in the case of liquefiable soils compared to non-liquefiable soils.

Large scale shake table studies have shown that the magnitude of liquefaction induced displacement depends on properties of liquefiable and non-liquefiable soil strata, pile properties like bending and stiffness strength, pile cross sectional area and exposure of pile area to lateral pressure [10, 11]. Numerical studies on pile response to lateral spreading on different pile foundation models such as end bearing, floating piles, pile and pile group with and without pile-cap in two- and three-layer liquefiable soil have been reported, and the results indicate that the bending moment depends on the liquefiable soil and shallow non-liquefiable layers [12–15]. The maximum bending moment induced in the pile is due to the presence of a shallow non-liquefiable layer showing passive mode failure. The seismic behavior of piles under earthquake excitations in liquefiable soil is complex because of the gradual buildup of pore pressure and the corresponding decrease in strength and stiffness [16, 17]. Nguyen et al. [18] carried out dynamic centrifuge tests on a pile group embedded in sloping ground to assess the relationship between soil resistance and pile displacement.

Pile bending moment in liquefiable sites increases significantly in comparison to non-liquefiable sites due to dissipation of lateral support of the liquefied strata. The peak bending moment is noticed at the interface of liquefied and non-liquefied strata, and the inertial interaction between soil and pile provides the most bending moment at the top of the pile and at the interface of top clay and liquefied loose sand layers [19]. The bending moment reaches its highest value at the interface of liquefied and non-liquefied soil strata. The pile lateral displacement decreases considerably when the thickness of the liquefiable sand layer is decreased. Once the liquefiable layer becomes denser, the liquefied depth becomes shallower and the dynamic response of the pile reduces substantially. Soil deformation induced kinematic force is dominant in liquefiable sand, and superstructure induced inertial force is relatively insignificant [20].

Analytical studies [21, 22] have been performed to determine the influence of soil-pile-structure interaction in liquefiable soils and the influence of relative density and the position of a liquefiable soil layer on the buckling capacity of pile foundations. The behavior of a pile foundation depends on the structure mass, pile stiffness, soil density, acceleration of input motion, and slope of the ground [23]. The pile bending moment is maximal when the liquefiable soil deposit is 60% of the non-liquefiable soil layer.

Studies have shown that the design of piles should consider the effect of lateral spreading on sloping ground. Centrifuge and shake table studies permit detailed measurements of the response of the system under different earthquake characteristics such as level of shaking, frequency content, and superstructure characteristics. However, centrifuge tests pose a challenge in modelling sand particles. The pile response studies using centrifuge modelling, shake table and numerical modelling, including field observation, indicate complex soil-structure interactions with uncertainties requiring further study regarding the pile response in the case of sloping multi-layer liquefiable deposits. The effect of ground sloping on pile response during earthquake loading needs to be explored to quantify bending moment and shear force response for engineering design.

Lateral spreading can occur on gently sloping ground or on nearly flat ground adjacent to water bodies. However, if any structures are present, it can cause significant damage. Level ground liquefaction is caused by the upward flow of water owing to the dissipation of seismically induced excess pore pressure. This results in large, chaotic movements called "ground oscillations" during shaking, but produces little permanent lateral soil movement. It is of major concern when pile foundations are resting on sloping ground with a thick crust of non-liquefiable soil strata spread over the surface of liquefiable soil and piles are inserted into non-liquefiable soil beneath the liquefied soil.

Japanese Road Association (JRA) [24] guidelines quantify the lateral pressure on pile due to the flowing liquefied soils as a result of the overburden pressure and this lateral pressure is taken as 30% of the overburden pressure at that depth. During 1995 kobe earthquake, Tokimatsu and Asaka [11] have reported that pile foundations will fail even in case of level grounds similar to that observed in laterally spreading ground. The extensively used example of failure of Showa bridge after 1964 Niigata Earthquake which was actually used to demonstrate the effect of lateral spreading loads on pile foundations designed using the codal provisions of JRA [24] shown by Bhattacharya et al. [25] that piles are safe against the JRA codal provisions of 1996 collapsed even though the code was revised several times after the earthquake. Hence, there is need for better understanding as some observations of pile failure might not be described based on the present hypothesis. Therefore, the present study examines the influence of liquefiable soils on the seismic performance pile foundations in sloping ground conditions and associated lateral spreading under dynamic loading [26]. To achieve this goal, a three-dimensional explicit finite difference program, FLAC3D [27] software (Itasca, 2012) is used to develop the numerical model and carry out simulations to evaluate the performance of piles under varying sloping ground

conditions. The conclusions reached will help practicing engineers to have better understanding of piles resting in liquefiable soils and provide an optimized design. The methodology followed for the study is presented in the form of a flow chart shown in Figure 1.

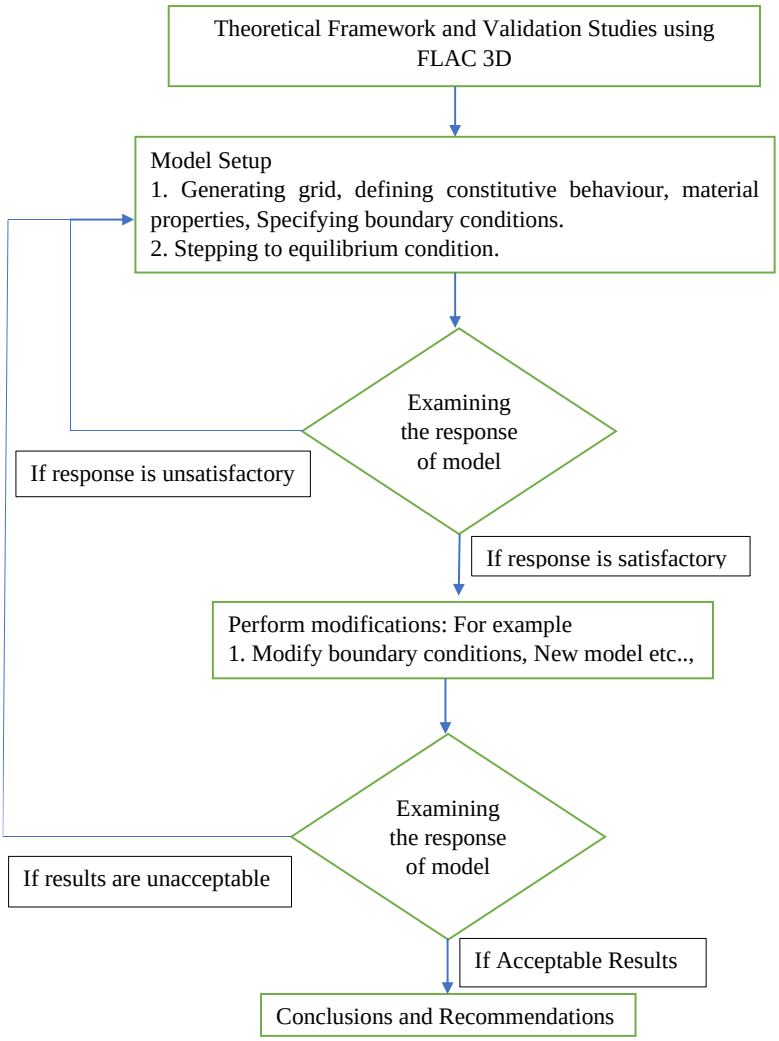

Figure 1. Methodology followed for the study

2. Validation Study

In order to carry out the detailed parametric studies, it is proposed to validate a study from previous literature. Hence, centrifuge model study by Abdoun et al. (2003) [3] has been considered and validated using finite difference program, FLAC3D.

2.1. Constitutive Model

The soil stress-strain behavior is considered as elasto-plastic in nature and Mohr-Coulomb constituent model was chosen to model non-liquefiable Slightly Cemented Sand (SCS) strata. Failure envelope for the constituent model corresponds to Mohr-Coulomb criterion with tension yield function. The location of stress point on failure envelope is controlled by non-associated and associated flow rule for shear and tension failure. The liquefiable soil i.e. Nevada sand (Nsand) layer is simulated by using the Byrne (1991) [28] model to consider pore water pressure effect. The empirical equation (Equation 1) relates the change in volume ($\Delta\varepsilon vd$) to the corresponding cyclic shear strain amplitude (γ):

$$\frac{\Delta\varepsilon vd}{\gamma} = C_1 \exp\left(-C_2\left(\frac{\varepsilon vd}{\gamma}\right)\right) \quad (1)$$

The parameter C_1 governs the amount of change in volume and C_2 governs the shape of overall change in volume with number of cycles. In several cases, C_2 = 0.4/ C_1 so that Equation 1 becomes one parameter dependent equation. Byrne (1991) [28] stated that the constant, C_1 can be obtained from relative density, D_r, in percentage as in Equation 2. The constants used in this study are C_1=0.27 and C_2=1.47 for soil having D_r =40 %.

$$C_1 = 7600(D_r)^{-2.5} \quad (2)$$

2.2. Soil-Pile and Pile cap Modelling

The pile is modelled as two noded finite structural elements (pileSELs) which has six degrees of freedom for each node. The pile interacts with surrounding soil through normal and shear coupling springs and these springs transmit the forces and motions between the soil grid and pile-pile cap. The interactions are represented by normal stiffness (K_n) and shear stiffness (K_s) and are given by Equations 3 and 4 respectively. Here, G is shear modulus of soil (GPa), r is pile radius (m) and μ= soil Poisson's ratio.

$$\textit{Normal Stiffness, } K_n = \frac{4Gr}{1-\mu} \quad (3)$$

$$\text{Shear Stiffness, } K_s = \frac{32(1-\mu)Gr}{7-8\mu} \quad (4)$$

Pile-cap was modeled as the assemblage of liner structural elements (linerSELs). LinerSELs are three noded flat finite elements. The interaction between the soil and pile-cap are modeled using normal spring stiffness (K_n) and shear spring stiffness (K_s) values are calculated using the following equation (Equation 5):

$$K_n = K_s = \frac{K+\frac{4}{3}G}{\Delta Z_{min}} \quad (5)$$

Here, K and G are taken as bulk modulus and shear modulus of soil respectively and ΔZ_{min} is least dimension of neighboring zone in the soil block. To prevent the input wave motion from getting reflected at boundaries of generated model, a free field boundary condition was applied at the edges of the generated model which absorbs and transmits the seismic waves through the model.

A validation study has been carried out by comparing the centrifuge model test results of Abdoun et al. (2003) [3] with finite difference analysis using FLAC 3D. The centrifuge model [3] was inclined at 2° with the horizontal in which the vertical single pile is subjected to strong base shaking at a centrifugal acceleration of 50g, simulating a submerged ground slope containing model soil that represents 6 m thick prototype liquefiable sand layer and 2 m thick non-liquefiable stratum placed on above and below the liquefiable soil as shown in Figure 2-a. The model pile had an actual prototype diameter of 0.6 m and 10 m length. The soil layer thicknesses in Figure 2-a are in actual prototype model units and in the rest of this paper, all dimensions are shown in prototype units. The liquefiable layer constitutes uniform, fine Nevada sand with 40% relative density (D_r). The top and bottom layers are slightly cemented sand (SCS) representing non-liquefiable strata.

A rectangular (2.5×2.5 m) pile cap made out of aluminum with a thickness of 0.5m was rigidly connected to the pile made of Polyetherimide rod, embedded at the center of soil block. The centrifuge test model along with generated FLAC 3D model is shown in Figures 2-a, and 2-b respectively. The parameters considered for the pile, soil and pile cap are presented in Table 1. The model was excited with input base acceleration consisting of constant acceleration having prototype amplitude of 0.3g and 2 Hz frequency as shown in Figure 3. The values of normal and shear stiffness are calculated using Equations 3 and 4 are 6.4×10^6 N/m and 5.76×10^6 N/m respectively. The interaction between the pile cap and the soil which is obtained using Equation 5 is found to be 89.73×10^7 N/m.

Figure 4 shows the similarity in variation of bending moment with depth between centrifuge test and present FLAC3D modelling. The peak values of bending moment developed in pile near the top and bottom interfaces which is obtained from FLAC 3D are 125 and 138 kNm respectively. The values from centrifuge model tests are 130 kNm and 150 kNm respectively. Thus the results obtained from FLAC 3D compares well with centrifuge experimental test results.

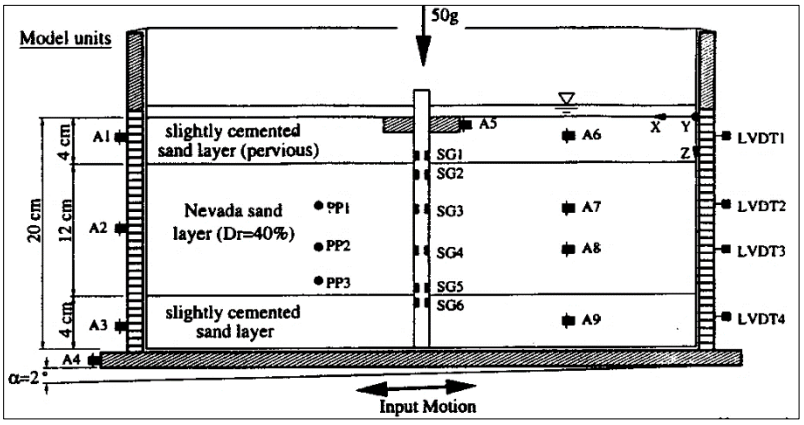

(a) Centrifuge test model [3]

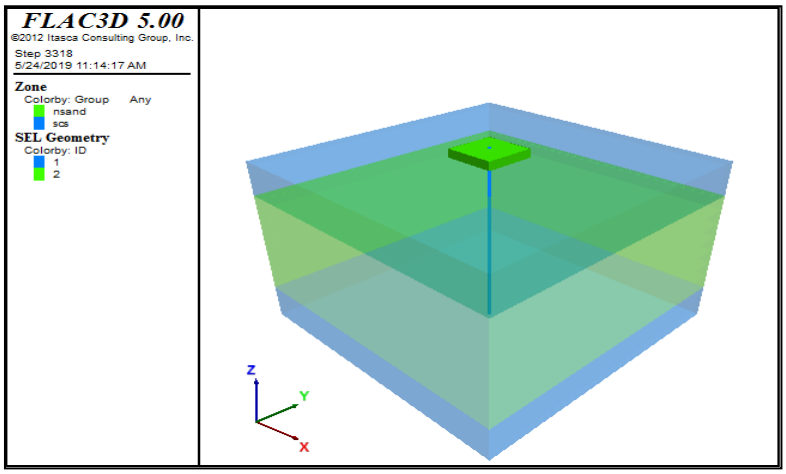

(b) FLAC 3D model

Figure 2. Soil pile model chosen for the present study

Table 1. Summary of material parameters considered [3, 29]

Parameters	Soil type		Pile structural element	Pile cap
	Nevada sand	Slightly cemented sand	Polyetherimide	
Cohesion (kPa)	-	5.1	-	-
Density (kg/m^3)	1800	1900	1270	2830
Friction angle [φ] (°)	30	34.5	-	-
Poisson's ratio [μ]	0.25	0.3	0.36	0.35
Relative density [Dr] [%]	40	-	-	-
Modulus of Elasticity (MPa)	10	60	1260	69000

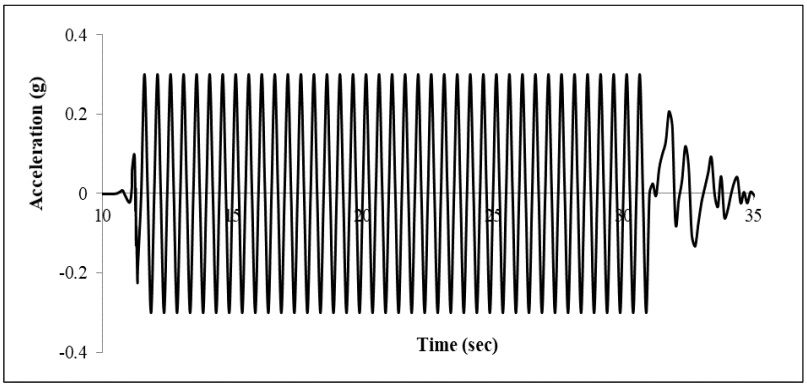

Figure 3. Harmonic ground motion [3]

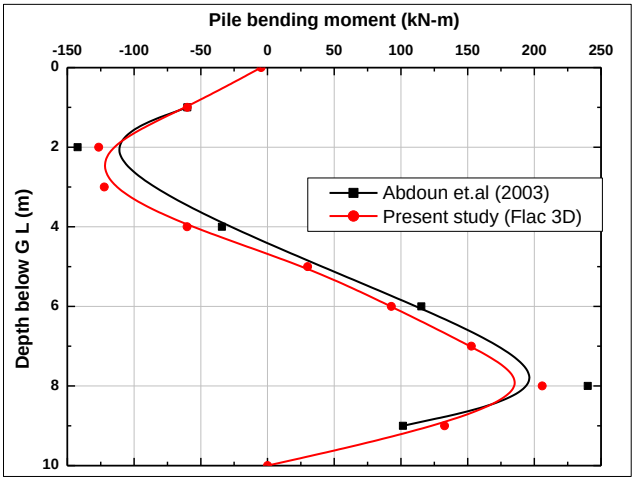

Figure 4. Comparison of bending moment with depth

3. Parametric Studies

3.1. Soil-Pile Model in Liquefiable Sloping Ground under Seismic Loading

Response analysis for the end bearing pile connected to the cap of dimension 2.5×2.5×0.5 m with floating pile head condition as depicted in Figure 5 is placed at the center of soil profile having a gentle slope of 2^o with horizontal. Since the soil model has a slope of 2^o with horizontal, the thickness of soil on one side is 10m and the other side is 10.52 m. The base of the soil model was subjected to harmonic motion of 0.3g acceleration (Figure 3), 2001 Bhuj (India) Earthquake with Peak Ground Acceleration (*PGA*) of 0.103g and 1940 El Centro Earthquake ground motions with PGA of 0.20g as presented in Figures 6-a and 6-b. The various parameters of soil, pile and Pilecap considered from literature [3, 29] are shown in Table 1. The response of pile to harmonic, 2001 Bhuj earthquake and 1940 El Centro earthquake ground motion are compared and reported. Figure 7-a shows the pile deflection with depth. The maximum pile displacement is obtained at the top. Figure 7-b shows the bending moment variation in pile with depth. Highest bending moment is noticed at the interface between liquefiable and non-liquefiable layers. Figure 7-c represents the change in shear force along the pile length. The peak value of shear force is observed at the top and at 5m depth below the ground level, it is observed that the forces are negative.

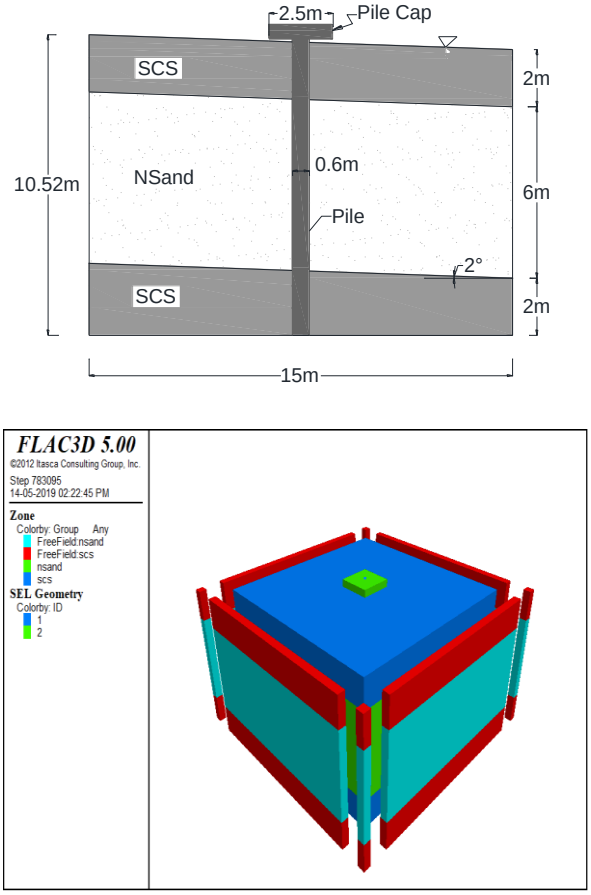

Figure 5. Typical soil pile model

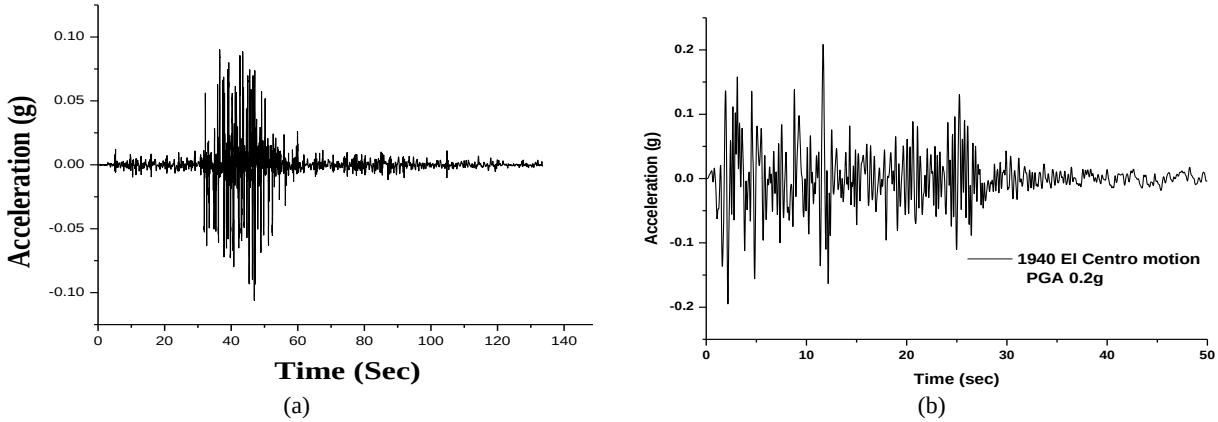

Figure 6. Earthquake ground motions (a) 2001 Bhuj earthquake (b) 1940 El Centro earthquake

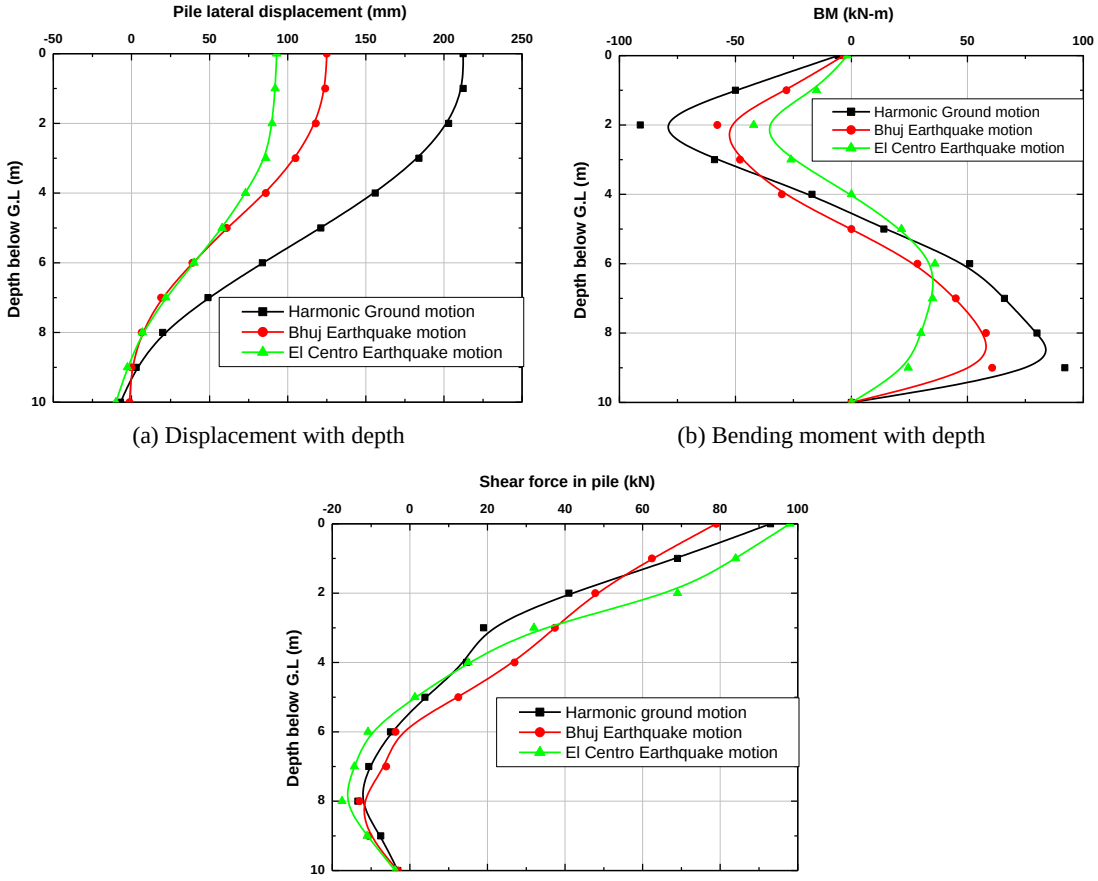

(a) Displacement with depth

(b) Bending moment with depth

(c) Shear force with depth

Figure 7. Pile response under different earthquake loadings

3.2. Lateral Spreading of Ground under Harmonic Ground Motion

The lateral ground displacement at the ground level and at the top interface (2 m from top) was measured at a section along a-a, b-b and c-c as shown in Figure 8 for harmonic motion (Figure 3). The ground displacement is measured from the inward side of pile to outward side of pile at the ground level and at the top interface. Figure 9-a shows lateral ground displacement versus horizontal distance at the ground level along section a-a, b-b and c-c. On the front side (Inward side) of pile, ground displacement is 325 mm at 3 m, remains constant till 7.5 m and at 14 m, it reduces to 90mm. It was noticed that existence of pile acts as barrier resulted in reduced pile displacement on the outer side. Further the lateral ground movement (325 mm) is more compared to the pile movement at the top (213 mm) (Figure 7-a). Figure 9-b shows the ground displacement versus the horizontal distance from the inward side at the top interface (i.e. 2 m from top) along section a-a, b-b and c-c. In the front side, ground displacement along a-a and c-c is increasing from 3m to reach maximum value of 825 mm at 10 m distance and reduced to 598 mm at 14 m from the inward side respectively. It was noticed that along b-b at a distance of 3 m, the displacement value is very small in comparison to section a-a, and c-c. Again the presence of pile acts as a barrier and the displacement reduces rapidly till 8 m distance and the maximum value of 74 mm is obtained at 10 m. Further at 14 m distance, the displacement reduces to 589 mm. At the top interface, the lateral ground movement (100 mm) is less compared to pile displacement (203 mm) (Figure 7-a, at 2 m depth).

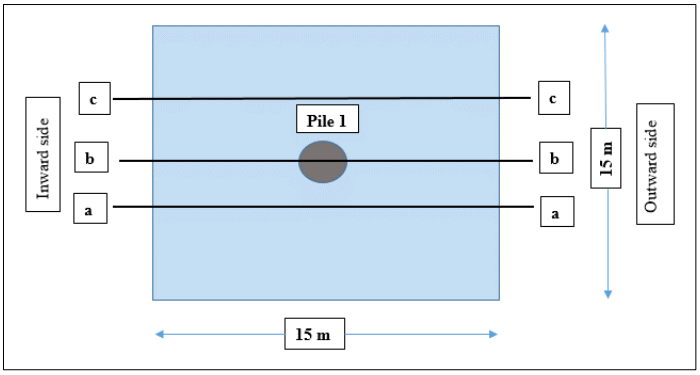

Figure 8. Plan of soil model showing sections along which ground displacements are measured

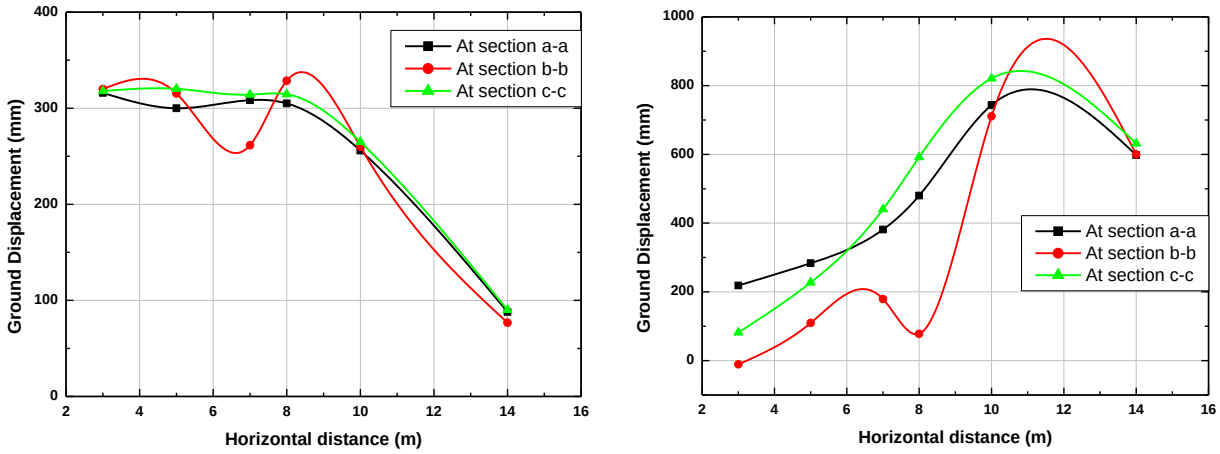

(a) At ground Level (b) At top interface level

Figure 9. Variation of Ground displacements with distance

Figure 10 shows the measured lateral ground displacement profile with depth wherein the free field lateral displacement at the ground level is 325 mm and at the top interface, it is 100mm and decreases gradually to zero at the pile tip. Similar observations were made by Abdoun et al. (2003) [3] during centrifuge test.

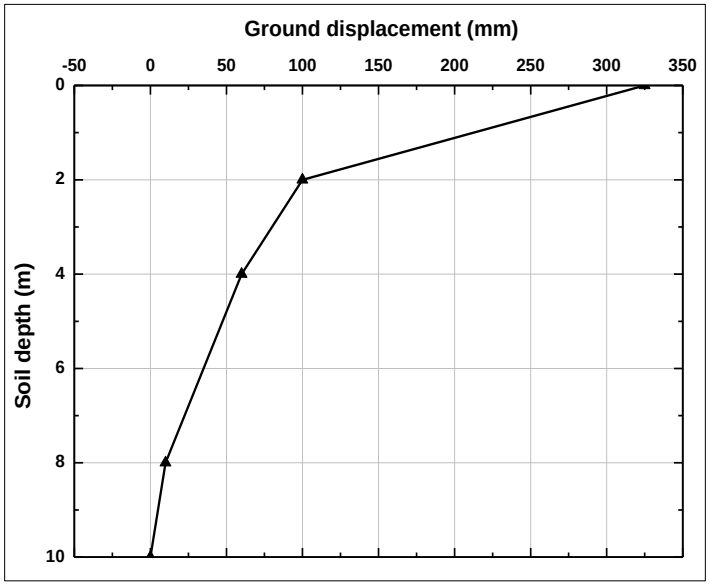

Figure 10. Lateral ground displacement profile with depth

3.3. Pile Group Behaviour in Liquefiable Sloping Ground under Harmonic Ground Motion

The analysis was further extended to study the behaviour of pile group model in liquefiable sloping ground under harmonic excitations. The simulation was done in two stages. In the first stage, the gravity loading was applied and the stress-strain values were set as initial values. This was followed by dynamic analysis performed by applying the ground motion at the base. Parametric study was carried out for a pile group under sloping ground having an inclination of 2° to 10° with horizontal. While modelling sloping ground, the bottom was kept horizontal and the respective slopes were maintained at interfaces and top layers.

The soil pile group model is shown in Figure 11-a and 11-b in which pile 1 and 2 are front piles, Pile 3 and 4 are rear end piles in x-direction. Figure 12-a, depicts the variation of lateral displacement of pile group at the top. It is evident that the displacement values are increasing with the increase in slope of the ground. The peak displacement for 0° slope (level ground) is 135 mm and for 10° slope, it is 548.4 mm. The pile displacement for 10° slope is about 4.5 times larger compared to level ground. Figure 12-b shows the variation of pore pressure ratio with depth for varying sloping angles. Due to dynamic loading, pore pressure builds up in the sand and the pore water pressure (PWP) ratio reaches to 100% (i.e., r_u=1) demonstrating complete liquefaction of sand layer.

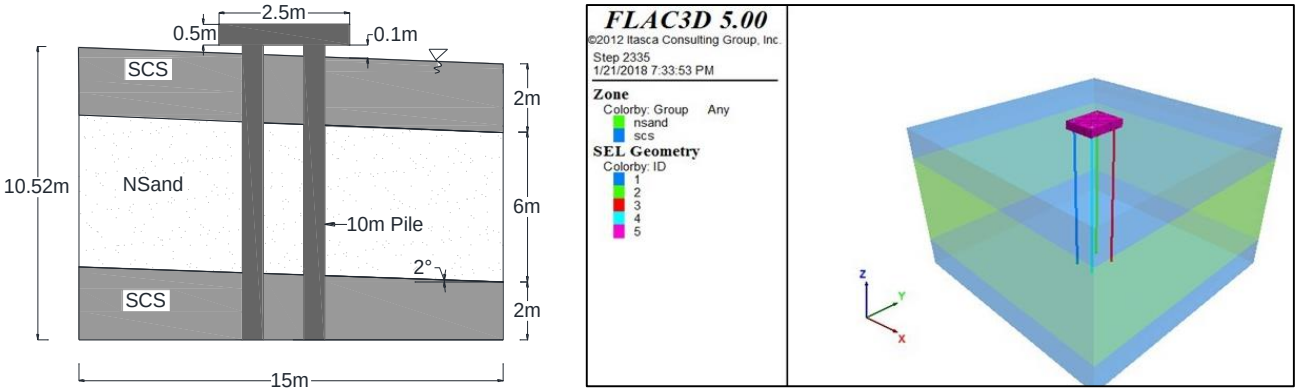

(a) Typical sketch of soil-pile group model (b) Three dimensional view of pile group model

Figure 11. Model of the soil pile group

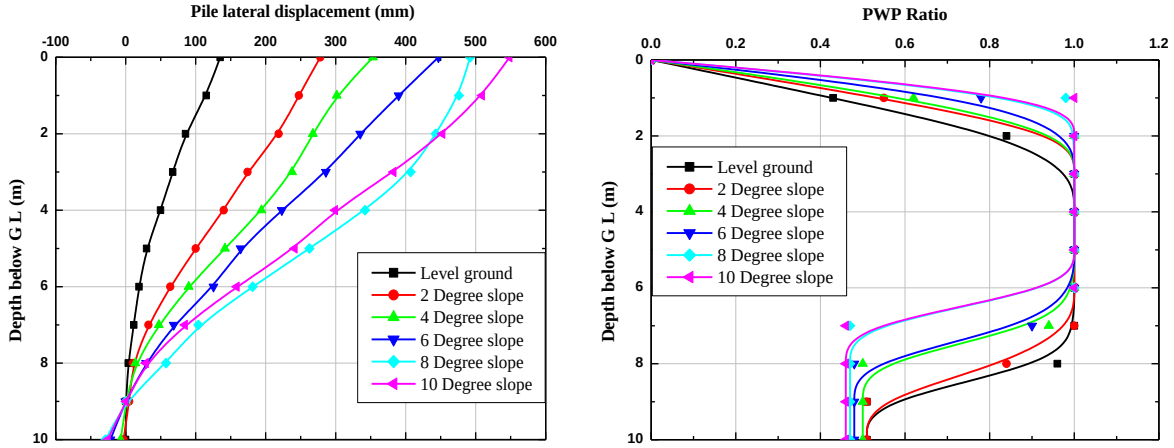

(a) (b)

Figure 12. (a) Pile displacement along the depth-(b) Pore water pressure Ratio with depth

Figures 13-a, and 13-b refers to bending moment variation of front and rear piles respectively. In the front piles due to bending, maximum moment appears at the bottom liquefiable and non-liquefiable soil interface. Bending moment values increases from 46.08 kN-m for level ground to 253.49 kN-m for 10° sloping ground, thereby the increase in bending moment is about 5.5 times for sloping ground compared to level ground. Similar responses were obtained for rear end piles also. The bending moment at bottom interface varies from -2.41 kN-m for level ground to 88.61 kN-m for 10° slope and near the top interface, the moment increases from 40 kN-m to 121 kN-m. The increase in bending moment is about 3 times in case of sloping ground compared to level ground. Therefore, the results clearly indicate that even a gentle slope of 2° would result in higher bending moment in piles at both the interfaces and this aspect needs to be considered carefully while designing the piles in sloping ground.

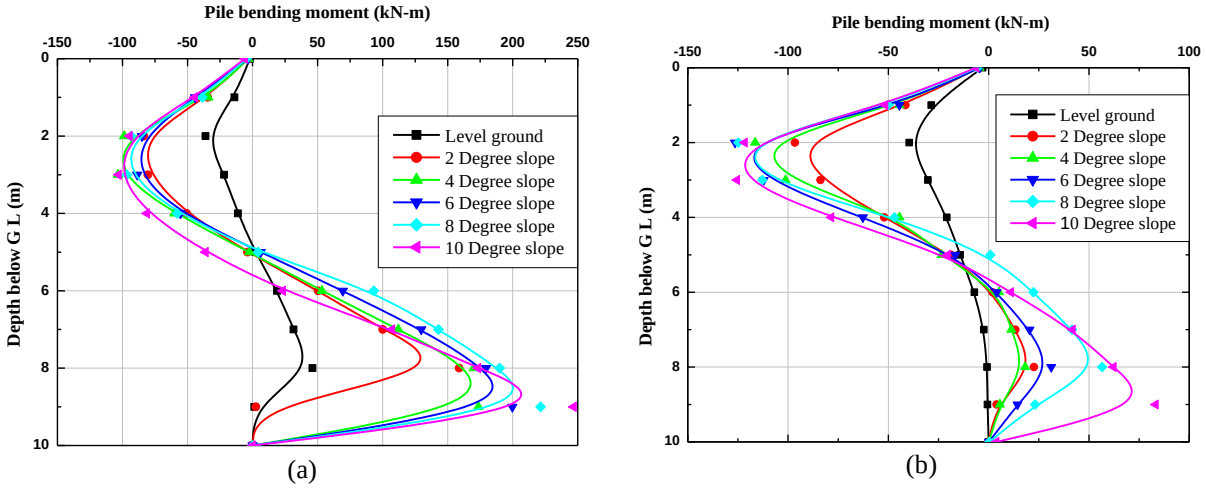

(a) (b)

Figure 13. (a) Bending moment in front Piles- (b) Bending moment in rear Pile

The variation of ground acceleration with soil depth has been measured at the ground level and near the interfaces as shown in Figure 14. It is clear that once the soil gets liquefied, it causes the spike in acceleration. From the given base acceleration of 0.3g (2.94 m/s^2), acceleration got amplified to 1.79g (17.55 m/s^2) at the bottom interface and similar spike has been observed at the top interface as well. At the surface level, an acceleration of 0.97g (9.53 m/s^2) is obtained. Figure 15 shows the acceleration-time history response at the ground level.

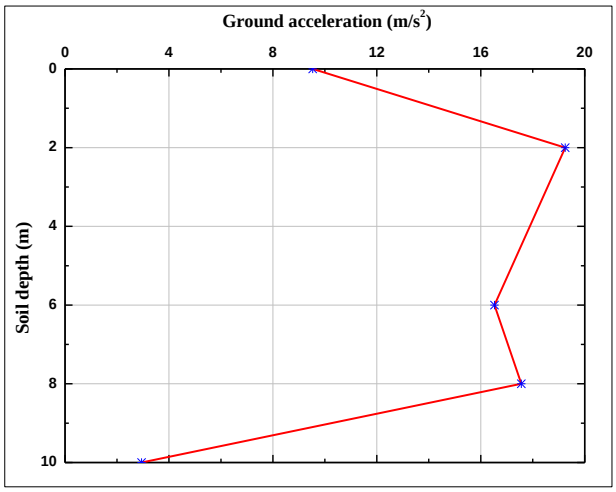

Figure 14. Measured ground accelerations at different depths

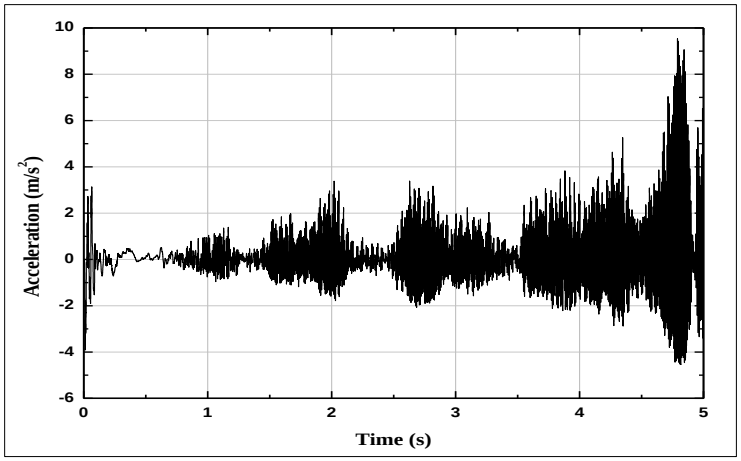

Figure 15. Acceleration response at the ground level

3.4. Lateral Spreading of the Ground under Harmonic Ground Motion

The ground displacement along the horizontal direction of shaking is measured at section A-A along the width of the soil profile and at sections 1-1 and 2-2 along the depth of ground as shown in Figure 15. Section A-A is considered at the center of soil mass (at 7.5 m). Section 1-1 and 2-2 are at the ground level and at the top interface (2 m from top) as shown in Figure 16 and Figure 17 shows the variation of ground and pile displacement for different sloping angles.

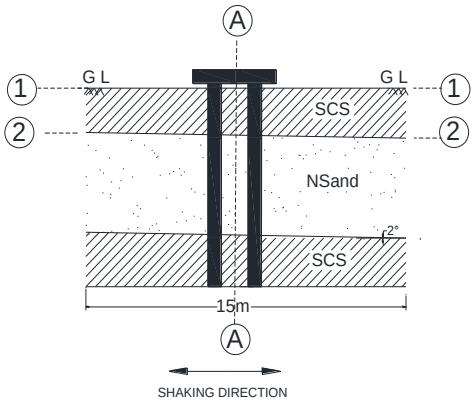

Figure 16. Sections along which the ground displacement is measured

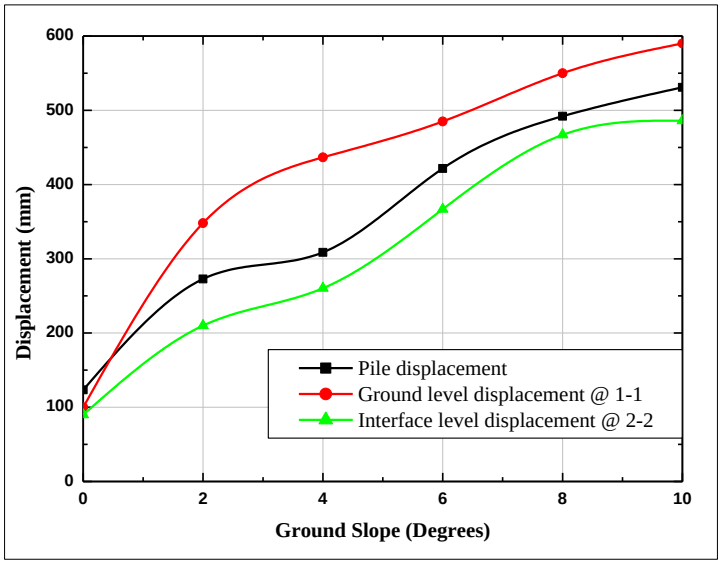

Figure 17. Variation of ground displacement for different ground slopes

From Figure 17, at section A-A, the maximum ground displacement at ground level and at the top interface is 590 mm and 486 mm, respectively, for 10^{o} slope. In Figure 16, the front piles and rear piles are situated at a distance of 6.75 m and 8.25 m, respectively, from the inward side. Within this enclosed area, the ground movement is reduced at the interface levels for every ground slope, owing to effective overburden pressure from the top non-liquefiable strata. Furthermore, the ground movement is greater compared to the pile displacement for all the sloping angles.

4. Conclusion

The present study proves the effectiveness of the numerical model in evaluating the response of piles to bending subjected to seismic loading. This study focused on the pseudo-static and kinematic facets of pile behavior during lateral spreading. Hence, no mass on top of the ground was considered in the analysis, and the results of pile displacement and bending moment reveal general consistency between previous studies and present numerical investigations. The stiff, non-liquefiable top layer is moving as a rigid body due to the liquefaction of the supporting stratum, thus causing the pile to deflect the maximum. Similar observations were made by Finn and Fujita et al. (2002). In all the cases of the present study, the peak values of bending moments considered throughout the length of piles appear at the boundaries of liquefied and non-liquefied soil layers, which is in close agreement with the theory and field observances.

The lateral loads and loads due to slope movement will make the pile unstable at much lower loads compared to axial loads. Although these lateral loads are secondary considerations to the basic necessity that piles in liquefiable soils must be examined for Euler's buckling load, the effect of lateral loads on piles needs to be considered carefully. The moment induced in the pile at the bottom interface for the front piles is 3 times greater compared to the rear piles and 1.25 times greater for the rear piles compared to the front piles for most of the sloping angles at the top interface. Similarly, the pile displacement increases with an increase in sloping angle, and for any slope angle, bending moment variation is linear with elevation within the liquefied layer. In addition, at the boundary of the liquefiable and non-liquefiable soil layers, plastic hinges are expected to form as the piles would experience the maximum bending moment. A recent study by Chavan et al. demonstrates that during initial liquefaction, the amplification of acceleration will occur at the interfaces of liquefiable and non-liquefiable soil layers. Similar observations are made in the present study. The results of the present work are restricted to the study of piles with pile caps in liquefiable soils without considering the external loads on piles from superstructure. Evaluation of pile response in liquefiable regions considers the parameters such as slenderness ratio of piles and thus check the stability of piles against Euler's buckling, deserves further study.

5. Declarations

5.1. Author Contributions

Conceptualization, G.M.B.; methodology, G.M.B.; validation, G.M.B. ; formal analysis, G.M.B.; investigation, G.M.B.; resources, G.M.B.; data curation, G.M.B.; writing—original draft preparation, G.M.B.; writing—review and editing, S.V.D., L.G., and R.R.B.; visualization, L.G.; supervision, S.V.D., and R.R.B.; project administration, L.G. All authors have read and agreed to the published version of the manuscript.

5.2. Data Availability Statement

The data presented in this study are available on request from the corresponding author.

5.3. Funding

The authors received no financial support for the research, authorship, and/or publication of this article.

5.4. Conflicts of Interest

The authors declare no conflict of interest.

6. References

[1] Abdoun, T., & Dobry, R. (2002). Evaluation of pile foundation response to lateral spreading. Soil Dynamics and Earthquake Engineering, 22(9–12), 1051–1058. doi:10.1016/S0267-7261(02)00130-6.

[2] Kaur, A., Singh, H., & Jha, J. N. (2021). Numerical Study of Laterally Loaded Piles in Soft Clay Overlying Dense Sand. Civil Engineering Journal, 7(4), 730–746. doi:10.28991/cej-2021-03091686.

[3] Abdoun, T., Dobry, R., O'Rourke, T. D., & Goh, S. H. (2003). Pile Response to Lateral Spreads: Centrifuge Modeling. Journal of Geotechnical and Geoenvironmental Engineering, 129(10), 869–878. doi:10.1061/(asce)1090-0241(2003)129:10(869).

[4] Finn, W. D. L., & Fujita, N. (2002). Piles in liquefiable soils: Seismic analysis and design issues. Soil Dynamics and Earthquake Engineering, 22(9–12), 731–742. doi:10.1016/S0267-7261(02)00094-5.

[5] Liu, L., & Dobry, R. (1995). Effect of Liquefaction on Lateral Response of Piles by Centrifuge Model Tests. In NCEER Bulletin, Issue January, 7–11. Available online: https://rosap.ntl.bts.gov/view/dot/13895 (accessed on December 2021)

[6] Nesrine, G., Djarir, Y., Khelifa, A., & Tayeb, B. (2021). Performance Assessment of Interaction Soil Pile Structure Using the Fragility Methodology. Civil Engineering Journal, 7(2), 376–398. doi:10.28991/cej-2021-03091660.

[7] Hamada, M., & O'Rourke, T. D. (1992). Case studies of liquefaction and lifeline performance during past earthquakes. Volume 1, Japanese Case Studies. Technical Rep. NCEER-92, 1, 1-28.

[8] Mizuno, H., & Iiba, M. (1982). Shaking table testing of seismic building-pile-soil interaction. In Proceeding of 8th World Conf. Earthquake Engineering, 649–656. San Francisco, United States.

[9] Phanikanth, V. S., Choudhury, D., & Reddy, G. R. (2013). Behavior of Single Pile in Liquefied Deposits during Earthquakes. International Journal of Geomechanics, 13(4), 454–462. doi:10.1061/(asce)gm.1943-5622.0000224.

[10] Tamura, S., & Tokimatsu, K. (2006). Seismic earth pressure acting on embedded footing based on large-scale shaking table tests. In Seismic performance and simulation of pile foundations in liquefied and laterally spreading ground, 83-96. doi: 10.1061/40822(184)8.

[11] TOKIMATSU, K., & ASAKA, Y. (1998). Effects of Liquefaction-Induced Ground Displacements on Pile Performance in the 1995 Hyogoken-Nambu Earthquake. Soils and Foundations, 38(Special), 163–177. doi:10.3208/sandf.38.special_163.

[12] Xu, R., & Fatahi, B. (2018). Effects of Pile Group Configuration on the Seismic Response of Buildings Considering Soil-Pile-Structure Interaction. In Q. T., T. B., & Z. Z (Eds.), Proceedings of GeoShanghai 2018 International Conference: Advances in Soil Dynamics and Foundation Engineering (pp. 279–287). Springer. doi:10.1007/978-981-13-0131-5_31.

[13] Russo, G., Marone, G., & Di Girolamo, L. (2021). Hybrid Energy Piles as a Smart and Sustainable Foundation. Journal of Human, Earth, and Future, 2(3), 306–322. doi:10.28991/hef-2021-02-03-010.

[14] Kwon, S. Y., & Yoo, M. (2020). Study on the dynamic soil-pile-structure interactive behavior in liquefiable sand by 3D numerical simulation. Applied Sciences (Switzerland), 10(8), 2723. doi:10.3390/APP10082723.

[15] Choudhury, D., Chatterjee, K., Kumar, A., & Phule, R. R. (2014). Pile Foundations during Earthquakes in Liquefiable Soils – Theory to Practice. 15th Symposium on Earthquake Engineering, 327–342. doi:10.13140/2.1.3796.3847.

[16] Lu, X., Mengen, S., & Wang, P. (2019). Numerical simulation of the composite foundation of cement soil mixing piles using FLAC3D. Cluster Computing, 22, 7965–7974. doi:10.1007/s10586-017-1544-6.

[17] Khalil, M. M., Hassan, A. M., & Elmamlouk, H. H. (2019). Dynamic behavior of pile foundations under vertical and lateral vibrations. HBRC Journal, 15(1), 55–71. doi:10.1080/16874048.2019.1676022.

[18] Nguyen, B. N., Tran, N. X., Han, J. T., & Kim, S. R. (2018). Evaluation of the dynamic p–y p loops of pile-supported structures on sloping ground. Bulletin of Earthquake Engineering, 16(12), 5821–5842. doi:10.1007/s10518-018-0428-3.

[19] Basavanagowda, G. M., Gowthami, P., Dinesh, S. V., Govindaraju, L., & Balareddy, S. M. (2021). Behavior of Pile Group in Liquefied Soil Deposits Under Earthquake Loadings. Lecture Notes in Civil Engineering, 120 LNCE, 139–150. doi:10.1007/978-981-33-4005-3_11.

[20] Jahed Orang, M., Motamed, R., Prabhakaran, A., & Elgamal, A. (2021). Large-Scale Shake Table Tests on a Shallow Foundation in Liquefiable Soils. Journal of Geotechnical and Geoenvironmental Engineering, 147(1), 04020152. doi:10.1061/(asce)gt.1943-5606.0002427.

[21] Huded, P.M., Dash, S.R., Bhattacharya, S. (2022). Buckling analysis of pile foundation in liquefiable soil deposit with sandwiched non-liquefiable layer. Soil Dynamics and Earthquake Engineering, 154, 107133. doi:10.1016/j.soildyn.2021.107133.

[22] López Jiménez, G. A., Dias, D., & Jenck, O. (2019). Effect of the soil–pile–structure interaction in seismic analysis: case of liquefiable soils. Acta Geotechnica, 14(5), 1509–1525. doi:10.1007/s11440-018-0746-2.

[23] Hussein, A. F., & El Naggar, M. H. (2022). Seismic behaviour of piles in non-liquefiable and liquefiable soil. Bulletin of Earthquake Engineering, 20(1), 77–111. doi:10.1007/s10518-021-01244-4.

[24] Japanese Road Association (JRA). (1996). " Seismic design specifications of highway bridges", Japanese Road Association, in Earthquake Resistant Design Codes in Japan, Japan Society of Civil Engineers, Tokyo, Japan.

[25] Bhattacharya, S., Bolton, M. D., & Madabhushi, S. P. G. (2005). A reconsideration of the safety of piled bridge foundations in liquefiable soils. Soils and Foundations, 45(4), 13–25. doi:10.3208/sandf.45.4_13.

[26] Chavan, D., Sitharam, T. G., & Anbazhagan, P. (2022). Site response analysis of liquefiable soil employing continuous wavelet transforms. Geotechnique Letters, 12(1), 1–11. doi:10.1680/jgele.21.00091.

[27] FLAC3D. (2022). Fast Lagrangian Analysis of Continuum's version 5.0. Itasca Consulting Group, Minneapolis, Minnesota, United States.

[28] Byrne, M. P. (1991). A cyclic shear-volume coupling and pore pressure model for sand. Second International Conference on Recent Advances in Geotechnical Engineering and Soil Dynamics, 47–55. University of Missouri, Missouri, United States.

[29] Bowles, J.E. (2001) Foundation Analysis and Design. 5th Edition, McGraw-Hill Companies Inc., Singapore.